

# TEXTURES OF SHEET IN AA3003 ALUMINUM ALLOY UNDER BIAXIAL STRETCHING

X. Y. WEN\* and W. B. LEE

*Department of Manufacturing Engineering,  
The Hong Kong Polytechnic University*

*(Received 6 March 2000)*

In this paper, the textures are determined under plane strain tension, nonequi-biaxial stretching and equi-biaxial stretching. The changes of the major texture components in the sheet are analyzed and discussed. It is found that under plane strain tension, the strength of the  $\{110\}\langle 112 \rangle$  component increases by more than four times followed by the  $\{110\}\langle 111 \rangle$ , whereas the fraction of  $\{112\}\langle 111 \rangle$  component falls gradually. In the sample deformed with a strain ratio intermediate between these of plane strain tension and equi-biaxial stretching, the textural change is relatively small. Under equi-biaxial stretching, there is a big increase in the  $\{110\}$  rolling plane components with the peak at  $\{110\}\langle 111 \rangle$  orientation. The strength of the other components falls rapidly (e.g.  $\{110\}\langle 112 \rangle$ ) or remains low (e.g.  $\{112\}\langle 111 \rangle$ ).

*Keywords:* Texture; AA3003 aluminum alloy; Biaxial stretching; Plane strain tension

## 1. INTRODUCTION

The plastic deformations of single crystals and polycrystals is based on the microscopic behavior of solid materials. Various models for plastic deformation of crystals have been proposed according to certain microscopic features of these crystals. The crystal orientation is one of the crystallographic characteristics that describe microplastic deformation of solid. Taylor (1938) formulated a model of polycrystal plasticity, based on the crystallographic nature of plastic deformation

---

\*Corresponding author.

and the assumption of homogeneous strain. The orientation changes in tension and compression for a FCC polycrystal with random orientation distribution can be predicted by use of the model. Pickus and Mathewson (1939) who used Taylor theory, explained the origin of rolling texture in face centered cubic metal.

Texture development under partially constrained deformation should therefore be primarily prescribed by crystal geometry; physical differences between materials enter only after symmetric orientations have been reached, and only in the absence of geometric orientation stability. Fuh and Havner (1989) proposed a theory of minimum plastic spin for finite deformation of crystals, consistent with loading conditions and constrains. Three families of multiple-slip configurations of f.c.c. crystals were comprehensively investigated: (i) pure plane strain compression with a [100] axis of free extension; (ii) (110) loading in channel die compression; and (iii) all multiple-slip orientations in uniaxial tension. Panchanadeeswaran and Field (1995) focus upon the development of deformation textures in aluminum during this type of processing. Daniel *et al.* (1993) had investigated the texture evolution induced by tensile deformation and deep drawing. The results indicate that the initial texture changes drastically after a few percent of plastic strain and evolves towards a single orientation for which the  $\langle 110 \rangle$  direction is aligned with the tensile or drawing axis. The ideal orientations of rolling textures for f.c.c. metals are investigated by Zhou *et al.* (1996). Analytical solutions for the stress states, slip distributions and lattice spins are obtained using both a rate-sensitive crystal plasticity model and the classical Bishop and Hill (1951) theory. It is shown that, in the limit of zero strain-rate sensitivity, the analytical rate-sensitive results turn to those of the Bishop and Hill theory. Furthermore, all of the possible Bishop and Hill slip systems turn out to be active in the limiting rate-sensitive solutions. Using a rate-sensitive crystal plasticity model together with the full constraint Taylor theory, Zhou and Neale (1994) investigated the formation of textures during biaxial stretching of FCC sheet metals. The investigation discloses the paths of orientation development and respective stable orientations, as well as the relation between the evolution paths and the biaxial strain ratio. The behavior of f.c.c. sheet metals having rolling textures was simulated under biaxial stretching conditions by Zhou and Neale. A rate-sensitive crystal plasticity model together with the full-constraint Taylor theory is used. Closed-form analytical

solutions were obtained for the stress states, slip distributions and lattice rotation fields at these ideal orientations of f.c.c. rolling textures. Under equi-biaxial stretching, the change of texture was studied by Lee *et al.* (1990). However, under nonequi-biaxial stretching, the development of texture was investigated very little.

## 2. MATERIALS AND EXPERIMENTS

The material used was an AA3003 aluminum alloy containing 1.09% Mn, 0.47% Fe and 0.15% Si with minor constituents 0.012% Zn, 0.024% Ti, 0.003% Mg and 0.095% Cu. One sheet was DC cast and hot rolled to 9.94 mm thickness, and then the sheet was hot rolled to 2.5 mm and heat treated.

### 2.1. Plane Strain Tension

An approximate state of plane strain is created in a wide sheet which is pulled in between two cross-heads in a tensile testing machine. If the lateral spread is small in comparison with the reduction in thickness, the sheet is deformed under an approximately plane strain condition, with the exception of narrow zones near the edges. Samples of the plane strain tensile test were prepared from a 2.5 mm thick hot rolled sheet. The size and shape are shown in Figure 1. Tensile tests were carried out on a MTS Testing Machine at a cross-head speed of 5 mm/min. The major strains,  $\epsilon_{11}$ , employed are listed in Table I. The samples were stopped in eight strain levels under the plane strain test, and the sample was deformed to fracture.

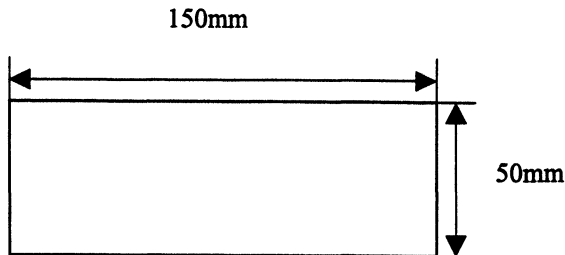


FIGURE 1 Sample for the plane strain tensile test.

TABLE I Strain values under plane strain tension

Sample No.	Pst0	Pst1	Pst2	Pst3	Pst4	Pst5	Pst6	Pst7	Pst8
$e_{11}$ (%)	0	5.10	12.2	15.6	20.5	25.8	28.6	31.7	34.3

## 2.2. Biaxial Stretching

The thickness of samples used for the equi-biaxial stretching test was 2.5 mm. The size and shape of the samples are designed and illustrated in Figure 2. The samples were stretched to five different strain levels in equi-biaxial stretching, and six different strain levels in nonequi-biaxial stretching on a two axes testing machine. For equi-biaxial stretching, the speed of the two cross-heads was set at 5 mm/min. For nonequi-biaxial stretching, the cross-head speed of the  $X$ -axes was  $v_{11} = 5$  mm/min and  $Y$ -axis was  $v_{22} = 3$  mm/min. The major strain and minor strain of each sample were recorded by the use of an instant grid method, and are shown in Tables II and III.

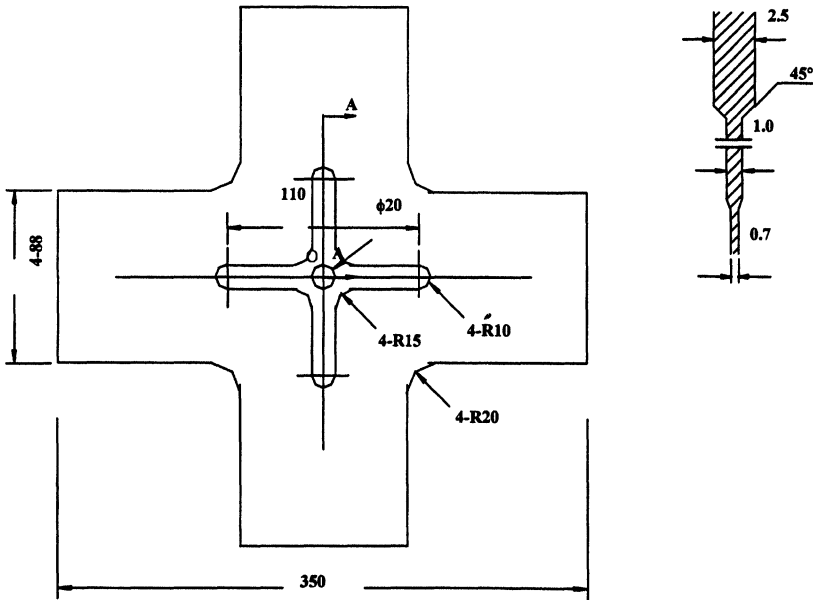


FIGURE 2 Sample size and shape for biaxial stretching (mm).

TABLE II The major strain and minor strain of samples in equi-biaxial stretching

<i>Equi-biaxial stretching (<math>v_{22}/v_{11} = 1</math>)</i>						
<i>Sample No.</i>	<i>EB0</i>	<i>EB1</i>	<i>EB2</i>	<i>EB3</i>	<i>EB4</i>	<i>EB5</i>
$e_{11}$ (%)	0	5.25	5.87	7.20	7.74	18.03
$e_{22}$ (%)	0	4.00	5.08	6.00	7.54	11.82

TABLE III The major strain and minor strain of samples in nonequi-biaxial stretching

<i>Nonequi-biaxial stretching (<math>v_{22}/v_{11} = 0.6</math>)</i>							
<i>Sample No.</i>	<i>NB0</i>	<i>NB1</i>	<i>NB2</i>	<i>NB3</i>	<i>NB4</i>	<i>NB5</i>	<i>NB6</i>
$e_{11}$ (%)	0	5.45	6.08	8.41	13.91	15.7	22.44
$e_{22}$ (%)	0	2.29	5.20	5.40	6.00	6.49	7.04

**2.3. Measurement of the Pole Figures and Calculation of the Orientation Distribution Function**

Three incomplete  $\{111\}$ ,  $\{200\}$  and  $\{220\}$  pole figures were collected on a Phillips Dual X'pert XRD Systems (PW3710) for each sample. The tube electric current was 35 mA and the tube voltage was 40 kV. Roe's system was adopted and the orientation distribution function was

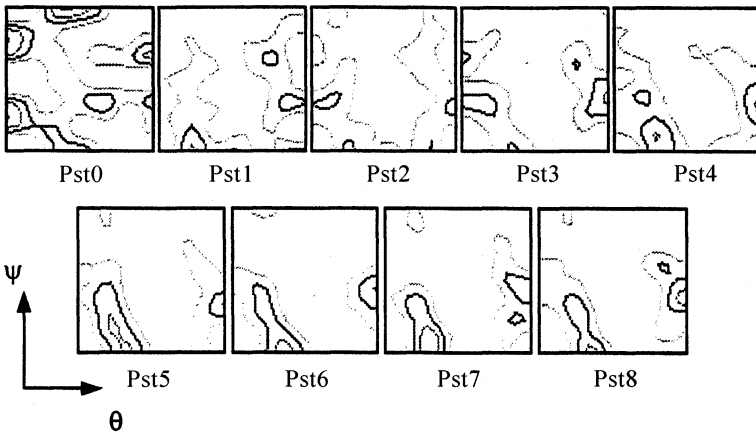


FIGURE 3 ODFs of the sheets (at constant  $\varphi = 45^\circ$ ) with various deformations after the plane strain tension.

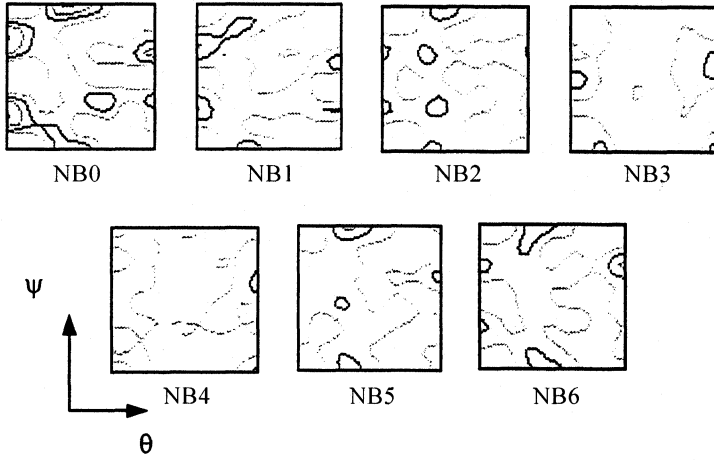


FIGURE 4 ODFs of the sheets (at constant  $\varphi = 45^\circ$ ) with various deformations after the nonequi-biaxial stretching.

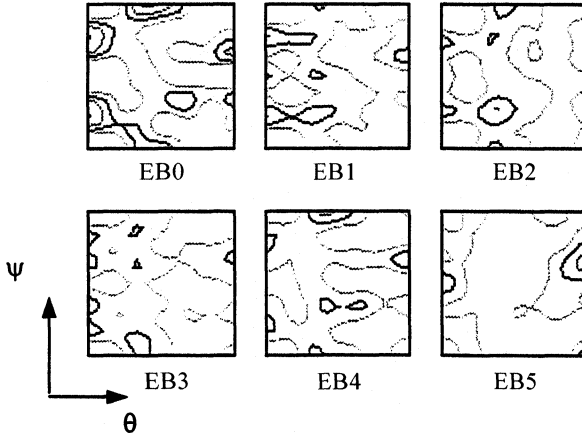


FIGURE 5 ODFs of the sheets (at constant  $\varphi = 45^\circ$ ) with various deformations after the equi-biaxial stretching.

calculated by using the software of Cai and Lee (1994) on an IBM/586 microcomputer (see Figs. 3 ~ 5). The volume percent of the major texture components in the sheet metal changes with strain under deformation (see Figs. 6 ~ 8).

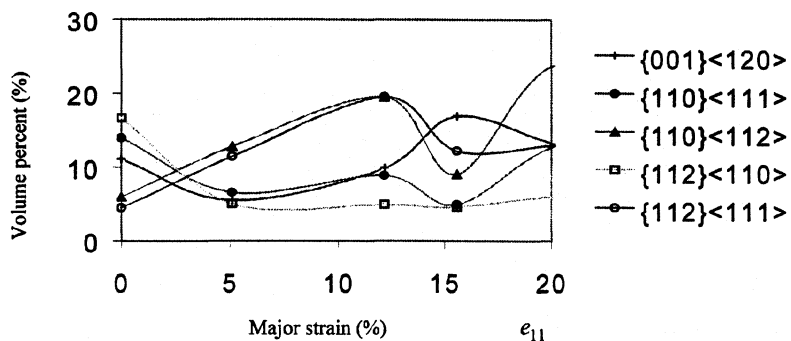


FIGURE 6 Percent of major texture components under plane strain tension.

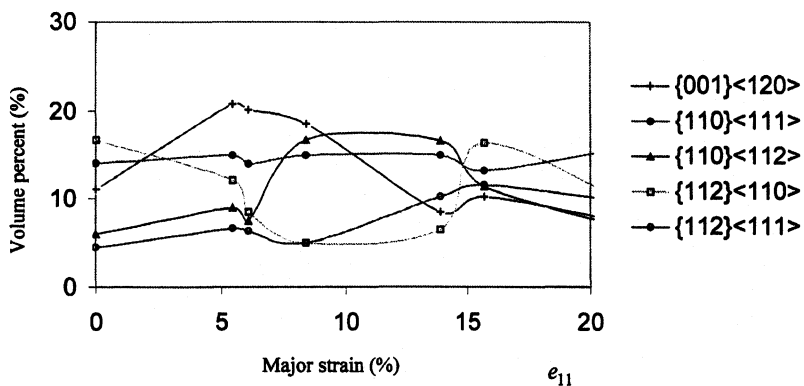


FIGURE 7 Percent of major texture components under nonequi-biaxial stretching.

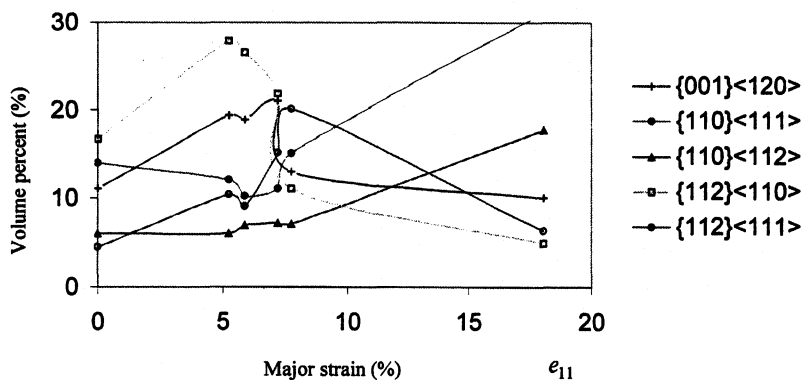


FIGURE 8 Percent of major texture components under equi-biaxial stretching.

### 3. THE RESULTS ANALYSIS AND DISCUSSION

The experimental pole figures and the calculated ODF of the sample sheet deformed under various stress states are shown in Figures 3 ~ 5. The starting textures of all samples are similar and the major texture components are  $\{001\}\langle 120\rangle$ ,  $\{110\}\langle 111\rangle$ ,  $\{111\}\langle 011\rangle$ ,  $\{112\}\langle 011\rangle$  and  $\{112\}\langle 111\rangle$ .

The change in the volume percentage of some major texture components of the sheet samples deformed under different strain rate ratios ( $\varepsilon_{22}/\varepsilon_{11} = 0, 0.6$  and  $1$ ) are summarized in Figures 6, 7 and 8. Comparing the samples, relatively large change is found in the texture formed under plane strain tension and equi-biaxial stretching. In the tensile sample, the strength of the  $\{110\}\langle 112\rangle$  component increases by more than four times followed by the  $\{110\}\langle 111\rangle$ , whereas the fraction of  $\{112\}\langle 111\rangle$  component falls gradually. In the equi-biaxial texture, there is a big increase in the  $\{110\}$  rolling plane components with the peak at  $\{110\}\langle 111\rangle$  orientation. The strength of the other components falls rapidly (*e.g.*  $\{110\}\langle 112\rangle$ ) or remains low (*e.g.*  $\{112\}\langle 111\rangle$ ). In the sample deformed with a strain ratio intermediate between these of tension and equi-biaxial stretching, the textural change is relatively small. The  $\{110\}$  fibre texture remains unchanged. Among all texture components, the cube  $\{001\}$  rolling plane components are found to decrease and remain weak from plane strain tension to equi-biaxial tension. Under nonequi-biaxial stretching, it is the characteristic of the changes in various texture components to increase or decrease between plane strain tension and equi-biaxial stretching.

Kohara (1981) measured the texture development in the equi-biaxial stretching of an aluminum sheet. The observed initial textures at the beginning of deformation comprised the S ( $\{124\}\langle 211\rangle$ ) plus Cube components. The texture obtained under equi-biaxial stretching could be represented by a  $\langle 110\rangle$ -fibre. Other minor components in the equibiaxial stretching texture were also present. The development of the Cube and the Copper orientations under equi-biaxial stretching has been simulated by Zhou and Neale (1994). The Cube orientation rotates to the Goss position and the Copper orientation rotates finally to the Brass position. The experimental equibiaxial textures obtained here conform with their predictions.

#### 4. CONCLUSIONS

- (1) Under plane strain tension, the strength of the  $\{110\}\langle 112\rangle$  component increases by more than four times followed by the  $\{110\}\langle 111\rangle$ , whereas the fraction of  $\{112\}\langle 111\rangle$  component falls gradually.
- (2) In the sample deformed with a strain ratio intermediate between these of plane strain tension and equi-biaxial stretching, the textural change is relatively small.
- (3) Under equi-biaxial stretching, there is a big increase in the  $\{110\}$  rolling plane components with the peak at  $\{110\}\langle 111\rangle$  orientation. The strength of the other components falls rapidly (*e.g.*  $\{110\}\langle 112\rangle$ ) or remains low (*e.g.*  $\{112\}\langle 111\rangle$ ).

#### *Acknowledgement*

The authors wish to thank the Research Grant Council of Hong Kong and The Research Committee of The Hong Kong Polytechnic University for the financial support of this project.

#### *References*

- Bishop, J. F. W. and Hill, R. (1951) *Phil. Mag.*, **42**, 414.  
Cai, M. J. and Lee, W. B. (1994) *Materials Science Forum*, **156–162**, 327.  
Daniel, D., Savoie, J. and Jonas, J. (1993) *Acta Met.*, **41**, 1907.  
Fuh, S. and Havner, K. S. (1989) *Proc. Roy. Soc. Lond.*, **A422**, 193.  
Kohara, S., Katsuta, M. and Aoki, K. (1981) *Japan. Inst. Light Met.*, **3**, 90.  
Lee, W. B., Chan, K. C. and Duggan, B. J. (1990) *Proc. Recrystallization 90*, Wollongong, Australia.  
Panchanadeeswaran, S. and Field, D. P. (1995) *Acta Met. Mater.*, **34**, 1683.  
Pickus, M. R. and Mathews, C. H. (1939) *J. Inst. Metals*, **64**, 237.  
Taylor, G. I. (1938) *J. Inst. Metals*, **62**, 307.  
Zhou, Y. and Neale, K. W. (1994) *Materials Science Forum*, **157–162**, 873.  
Zhou, Y., Neale, K. W. and Toth, L. S. (1996) *Textures and Microstructures*, **14–18**, 1055.